Thin Solid Films 704 (2020) 138026

Contents lists available at ScienceDirect

Thin Solid Films

journal homepage: www.elsevier.com/locate/tsf

Thermoelectric textile with fibers coated by copper iodide thin films

N.P. Klochko[a], K.S. Klepikova[a,*], D.O. Zhadan[a], V.R. Kopach[a], S.M. Chernyavskaya[a], S.I. Petrushenko[b], S.V. Dukarov[b], V.M. Lyubov[a], A.L. Khrypunova[a]

[a] National Technical University "Kharkiv Polytechnic Institute", 2, Kyrpychova str., 61002 Kharkiv, Ukraine
[b] Kharkiv National University named after V. N. Karazin, 4, Svobody Square, 61000, Kharkiv, Ukraine

ARTICLE INFO

Keywords:
Copper iodide
Thermoelectric generator
Textile
Crystal structure
Thin film

ABSTRACT

Here we obtained thermoelectric (TE) textiles on the base of the commercial cotton and polyester fabrics. For this we used deposition of copper iodide (CuI) thin films via low-temperature cheap and scalable method Successive Ionic Layer Adsorption and Reaction (SILAR). The TE textiles are comfortable to wear, breathable, nontoxic, light-weight, flexible and air-permeable. The CuI films in the TE textiles are composed of accreted flakes with nanoscale thickness (< 50 nm) or of nanowalls. Their crystal grains are less than 50 nm, contain a significant number of dislocations and an increased lattice parameter, and consequently have large compression microstrains. The TE textiles with CuI coated cotton and polyester have the Seebeck coefficients in the range of 120–180 μV K^{-1}, which are constant at the temperatures 290–365 K. The most effective single *p*-CuI thermoelectric leg has low internal resistance 2 kΩ. Its specific output power at temperature gradient 50 K is 31 μW/m^2. Three experimental flexible wearable TEGs of simple and affordable designs having each four thermocouples with *n*-Alumel and *p*-CuI thermoelectric legs on the thick cotton, thin cotton and polyester confirm the possibility of obtaining electricity using the developed TE textiles under conditions of temperature gradients from 5 to 50 K at near-room temperatures. The best TEG obtained on the polyester fabric has at temperature difference 50 K output TE characteristics: open circuit voltage 44 mV, short circuit current 1.3 μA, output power 16 nW. These characteristics remain unchanged after repeated bends of TEGs in the different directions.

1. Introduction

Recently, the rapid development of Internet of Things and miniaturized electronic devices have greatly increased demand for wearable power sources. Wearable thermoelectric generators (TEGs) that can, for example, convert body heat into electricity are promising for a powering of multifunctional devices for real-time health monitoring and activity tracking or meet individual cooling needs [1–13]. In addition, wearable thermoelectric devices can be used as self-powering thermoelectric (TE) sensors for a detecting temperature, pressure or strain [6,10–13]. Ideally, a wearable device should be comfortable to wear, breathable, nontoxic, light-weight, and even washable, for multiple uses [14–15]. To this end, an integration of thermoelectric materials with fabric is the most acceptable solution [1–13,16]. In particular, textile-based TEGs that can perpetually convert the ubiquitous temperature gradient (ΔT) between human body and ambience into electrical energy have attracted intensive attention to date [1–6,9,10,12,16]. In most designs, TE yarns, filaments or fibers are formed, which are then woven or inserted into fabrics [1,3,5,7,9,12]. These flexible thermoelectric yarns, fibers or filaments are mostly made by organic polymers or polymer/inorganic semiconductor composites, and also by organic polymer composites with carbon nanotubes (CNTs) or with graphene as fillers. They can be *n*- and *p*-conductivity type [1,9]. For instance, in [3] thermoelectric composites of poly(3,4-ethylene dioxythiophene)-poly(styrene sulfonate) (PEDOT:PSS) as *p*-type coating and polyurethane based composites with multi-walled CNTs of *n*-type were deposited directly on commercial polyester yarn via a dip coating method. The designed generator for the body heat conversion [3] has a sandwich structure similar to the classical inorganic TEG. This vertical (out-of-plane) type TEG allows generating of small temperature difference in the fabric thickness direction. Probably due to the short length of the thermoelectric legs, it generated low open current thermovoltage (V_{oc}) of ~800 μV and output power (P_{out}) of ~2.6 nW at ΔT = 66 K [3]. Vertical TEG for the harvesting of low-temperature waste heat was designed in [12] by sewing the thread filled by CNTs into a felt fabric. Its V_{oc} was 10 mV and P_{out} was ~8.5 nW at ΔT = 25 K.

* Corresponding address: Department of Materials for electronics and solar cells, National Technical University "Kharkiv Polytechnic Institute", 2, Kyrpychova str., 61002 Kharkiv, Ukraine.
E-mail address: catherinakle@gmail.com (K.S. Klepikova).

https://doi.org/10.1016/j.tsf.2020.138026
Received 26 December 2019; Received in revised form 30 March 2020; Accepted 10 April 2020
Available online 18 April 2020

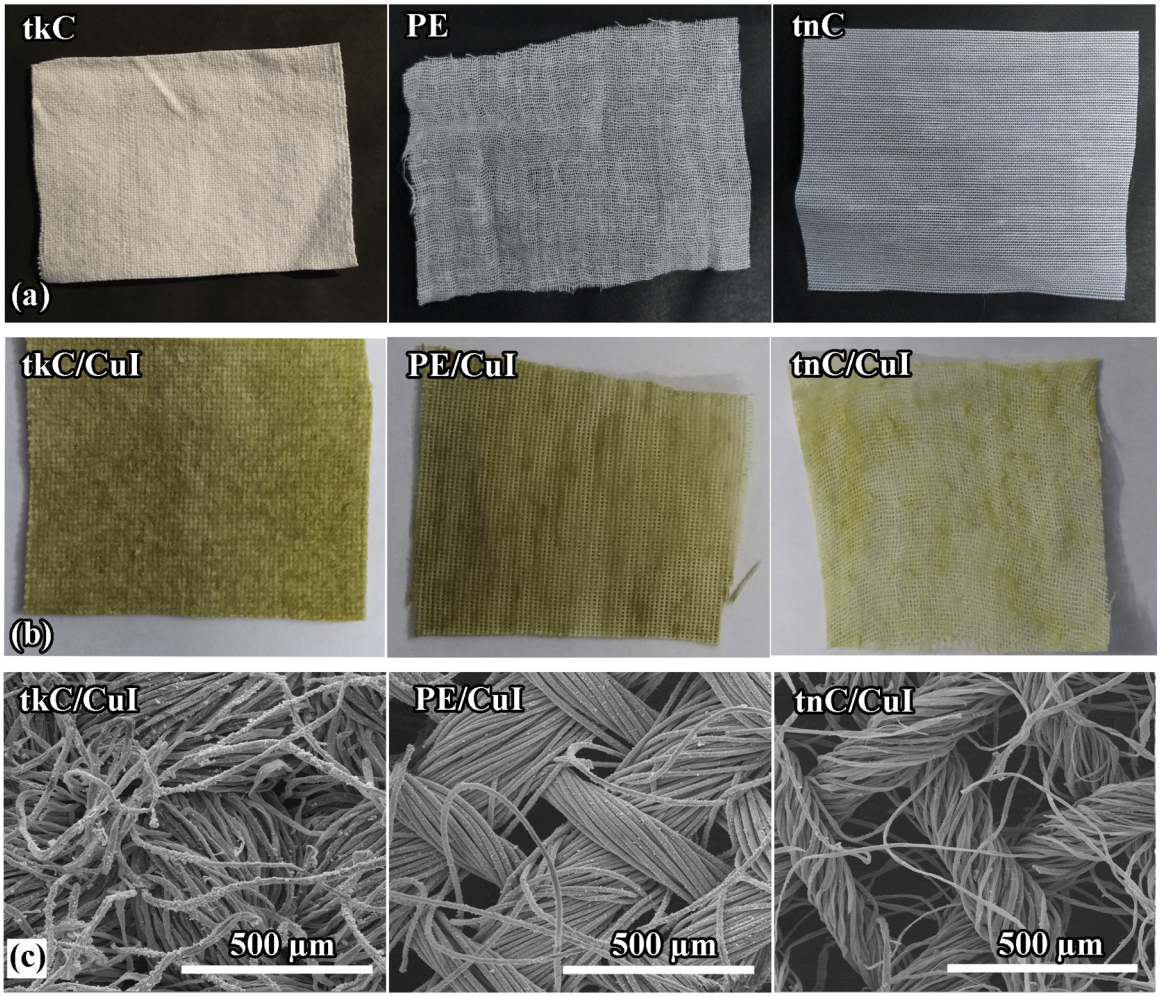

Fig. 1. Photos of thick cotton (tkC), polyester (PE), and thin cotton (tnC) fabrics (a) and of the corresponding CuI coated thermoelectric textiles tkC/CuI, PE/CuI, and tnC/CuI obtained through the deposition of CuI films via SILAR (b). (c)–SEM images of these thermoelectric textiles.

In [7] high-quality inorganic crystalline thermoelectric micro/nanowires of *p*-type $Bi_{0.5}Sb_{1.5}Te_3$ and *n*-type Bi_2Se_3 were obtained by means of thermally drawing method. They were hermetically sealed in borosilicate glass tubes with polymer coating. The resulting thermoelectric fibers with *p*-$Bi_{0.5}Sb_{1.5}Te_3$ and *n*-Bi_2Se_3 cores had high thermoelectric properties as their bulk counterparts. The hundreds of meters of continuous TE fibers were then woven into fabric to construct the wearable restructuring vertical TEG with mW/cm^2-level output power density through integration of a large number of *p*-*n* fiber pairs as thermoelectric legs. So, TEGs of vertical type based on textiles composed of different sets of TE fibers, filaments or yarns demonstrate excellent design flexibility, however, for their manufacture, a significant restructuring of the textile fabrication technology is necessary.

A much more technological approach is to create flexible in-plane TE devices by applying thin film thermoelectric semiconductors and conducting films as ohmic contacts to commercial textiles. According to [1,4,5,8,13,16], it is a cost-effective and practical way to add efficient thin film organic and inorganic conductive and semiconductor TE materials to fabrics. For example, in [1,5,16] in-plane TEGs were manufactured using PEDOT:PSS-coated strips of commercial polyester or cotton textile (*p*-type thermoelectric legs) connected with thin silver or constantan wires (*n*-type thermoelectric legs). For TEG with five pieces of polyester fabric strips and five Ag wires maximum P_{out} was 12.29 nW at ΔT = 75.2 K. For TEG comprising 5 pairs of *p*-*n* thermoelectric legs of PEDOT:PSS-coated cotton fabric strips and constantan wires, the V_{oc} of 18.7 mV and maximum P_{out} of 212.6 nW were generated at temperature difference of 74.3 K. In [13] a wearable highly stretchable self-powered temperature sensor was fabricated as knitted TE fabric using a commercially available knitted textile with a jersey structure composed of 80% 150-denier polyester and 20% 70-denier cotton and thermoelectric inks of PEDOT:PSS, silver nanoparticles (AgNPs), and graphene inks. The optimized sensor as in-plane thin film thermocouple fabricated with AgNPs and PEDOT:PSS coatings on the textile has linear temperature-sensing capability and generates V_{oc} of 1.1 mV for /ΔT = 100 K [13]. In [4] all-fabric TEG was created by vapor printing of persistently *p*-doped poly(3,4-ethylenedioxythiophene) (PEDOT-Cl) onto commercial cotton electrically connected with Ag paint and carbon fibers. TE textile has Seebeck coefficient of 16 µV K^{-1}. The P_{out} = 4.5 nW was generated at ΔT = 30 K. The Seebeck coefficient presented in [4] is rather low, that is the bottleneck for all known organic thermoelectric materials [1,3–5,9,13,16]. Moreover, authors [4,13] indicate the inconstancy of S in a small ΔT interval near room temperature for organic TE materials, which makes thermoelectric devices based on them difficult to control.

We were not able to find in the literature data on the manufacture of thin films of inorganic TE semiconductors on textile. The fabric-based flexible wearable thermoelectric devices presented recently in [1,2,8,11] were designed on the basis of thick films of inorganic semiconductors with a thickness from 11 µm to 395 µm [2,8], or contained TE pillars of 5 mm height of inorganic semiconductors [11], similar to the classical sandwich bulk TEGs. Authors [8] report scalable screen-printing of efficient inorganic 11 − 395 µm thick TE layers of

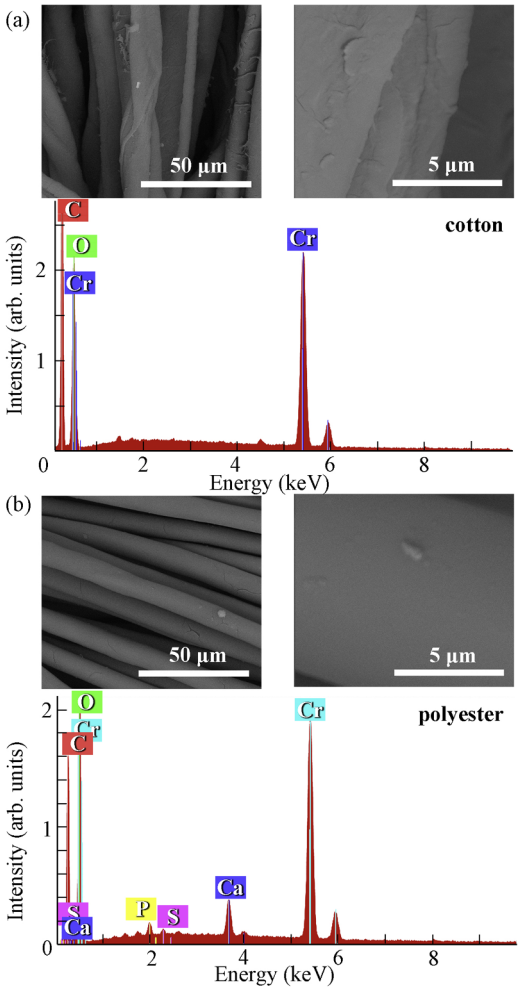

Fig. 2. SEM images and XRF data of the fabrics.

Table 1
X-ray fluorescence spectroscopy data of the fabrics.

Element	Cotton at. (%)	Polyester
C	60	46
O	40	52
Ca	–	< 1
S	–	< 1
P	–	< 1

Table 2
SILAR modes for making samples of thermoelectric textiles with fibers coated by thin CuI films.

Sample	Substrate	Anionic precursor, M NaI	Number of SILAR cycles
tkC/CuI_1	Thick cotton	0.05	40
tkC/CuI_2		0.075	
tkC/CuI_3		0.1	
tnC/CuI	Thin cotton	0.1	
PE/CuI_1	Polyester	0.05	
PE/CuI_2		0.075	
PE/CuI_3		0.1	
PE/CuI_4		0.05	80
PE/CuI_5		0.075	

semiconductor tellurides on a glass fabric using printing inks consisting of the particles *p*-type $Bi_{0.5}Sb_{1.5}Te_3$ or *n*-type $Bi_2Te_{2.7}Se_{0.3}$, binders, and organic solvents. The inability to replace glass cloth with commercial

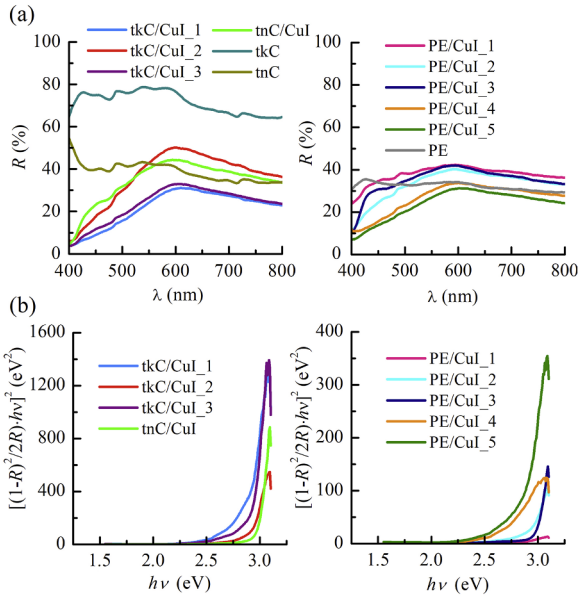

Fig. 3. Optical properties of the thermoelectric textiles with thick cotton (tkC), thin cotton (tnC) and polyester (PE) fibers coated by CuI films: (a) – diffuse reflectance spectra $R(\lambda)$; (b)–graphs for the CuI band gap finding by means of the Kubelka-Munk function.

cotton or polyester is associated with post-growth heat treatments. As it mentioned in [8], glass fabric lost porosity and breathability in areas coated with thermoelectric material. Moreover, as indicated in [2], notwithstanding glass fabrics have the feasibility to be fabricated in the form of clothing, specially designed fabric structures with large holes must be utilized to ensure the penetration of TE materials during screen-printing, which cannot be adapted to well-established weaving techniques.

The aim of the present work is to develop an approach for the fabrication of wearable fabric-based TEG which could combine the existing weaving techniques with promising inorganic thin film TE material copper (I) iodide (CuI) [15,17–22]. CuI is an environment friendly material composed of nontoxic and naturally abundant elements, and in its γ phase (γ-CuI) shows a *p*-type conductivity due to shallow acceptor level of copper vacancies [17–19]. According to [19], high thermoelectric performance in the wide band gap CuI is explained by its high value of *S* in the range from 123 μV K^{-1} [22] up to 207 μV K^{-1} [15,21] and high conductivity (with respect to the large band gap) from 7 × 10^2 Ω^{-1} m^{-1} [18] up to (2–5) × 10^3 Ω^{-1} m^{-1} [22] and 1.1 × 10^4 Ω^{-1} m^{-1} [15], as well as the low value of thermal conductivity. An important advantage of thin CuI films is the possibility of their manufacture on flexible polyimide [15], polyethylene naphthalate [19] and poly(ethylene terephthalate) [18–19,22] substrates, while maintaining the structure and TE properties when bending, which accompanied by stretching and compression of the films [15,18–19,22]. Different processes were successfully used for a production of the thermoelectric *p*-type γ-CuI thin films in [15,17–19]. Among them, vapor- and solid-phase iodination of Cu films obtained by resistive thermal evaporation [15,17], thermal evaporation of CuI powder [17], solid-phase iodination of reactively sputtered Cu_3N films [18], and reactive sputtering of CuI [19]. All these methods include the stage of vacuum deposition, so they cannot be considered as simple, cheap and affordable. Recently, we managed to obtain CuI thin films appropriate for use in TEGs via low cost, affordable and suitable for mass production chemical method Successive Ionic Layer Adsorption and Reaction (SILAR) carried out in aqueous solutions at room temperature [20–22]. In [20] SILAR method was used for a deposition of CuI thin films as TE material for vertical thermoelectric nanogenerator, which functioning (V_{oc} of 0.09 mV and P_{out} of 0.4 nW) carried out due

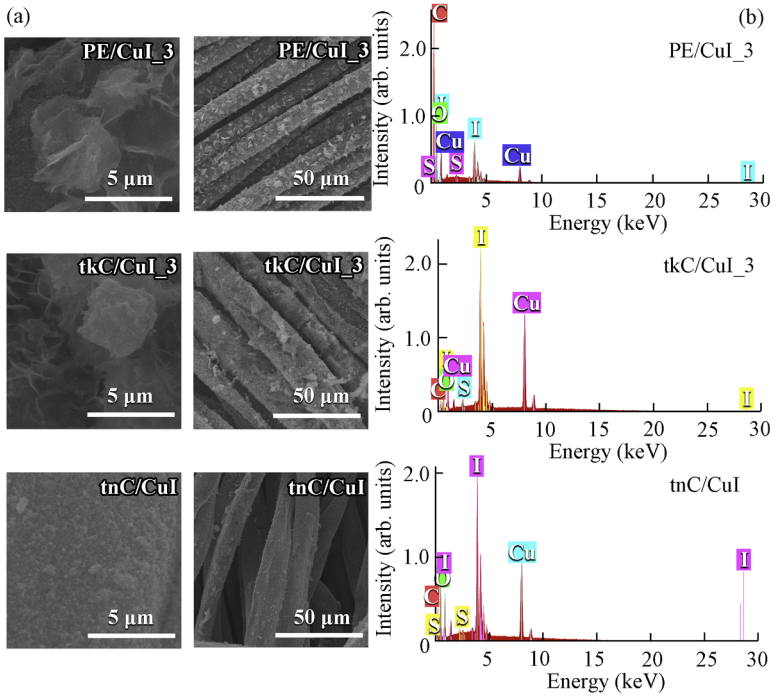

Fig. 4. SEM images (a) and XRF spectra (b) for three samples of thermoelectric textiles with CuI coatings obtained by means of 40 cycles of the SILAR method using anionic precursor 0.1 M NaI onto thick cotton (sample tkC/CuI_3), polyester (sample PE/CuI_3) and thin cotton (sample tnC/CuI).

Table 3
X-ray fluorescence spectroscopy data for all samples of the thermoelectric textiles.

Element	at. (%) in the thermoelectric textile sample on fabric								
	Cotton				Polyester				
	tkC/CuI_1	tkC/CuI_2	tkC/CuI_3	tnC/CuI	PE/CuI_1	PE/CuI_2	PE/CuI_3	PE/CuI_4	PE/CuI_5
Cu	13	26	28	14	<1	2	1	4	32
I	12	23	29	13	<1	1	1	3	27
C	47	31	27	44	67	65	68	62	24
O	28	20	14	29	31	32	30	31	14
S	–	–	<3	<1	<1	–	<1	<1	3

to a spontaneous temperature gradient ~7 K between uncoated area on the FTO substrate and the FTO area coated by CuI film, which occurs under an uniform heating of the entire device to 30 – 50 °C. In [21] CuI films with thermopower factor of 61.2 μW m^{-1} K^{-2} and the Seebeck coefficient of 207 μV K^{-1} were deposited via SILAR on glass substrates for thermoelectric conversion of near-infrared solar light in-plane TEG. Single *p*-type thermoelectric leg made with (0.5 × 3) cm^2 area CuI thin film can generate at near-room temperatures V_{oc} of 2.8 mV and P_{out} = 0.2 nW at ΔT = 15 K [21]. In [22] SILAR method has been used to create *p*-type CuI thermoelectric leg on poly(ethylene terephthalate) substrate for a new flexible wearable in-plane TEG. The obtained flexible CuI thin film single *p*-thermoelectric leg demonstrates at near-room temperatures output power of 17.1 μW/m^2 at the temperature gradient of 35 K [22].

Here, through the coating of CuI thin films via SILAR method onto commercial cotton and polyester fabrics we obtain different samples of thermoelectric textile. Due to the features of the SILAR method, it is possible to apply CuI thin films to all fibers on both sides and in the middle of the fabric, and even to form CuI nanoparticles inside the fibers, since aqueous solutions easily penetrate there. We study morphology, crystal structure and properties of the CuI coatings on the different textile fibers depending on the substrate material and on the SILAR mode. Output parameters of single *p*-type thermoelectric legs made from the different samples of CuI coated fabrics at near room temperatures investigated. Based on the experimental results, three most effective samples of these thermoelectric textiles selected. Then, experimental designs of lightweight, flexible and air-permeable wearable in-plane thermoelectric generators developed and manufactured, and output characteristics of these TEGs researched at ΔT in the range of 5–50 K.

2. Experimental details

In this study, to obtain samples of CuI coated thermoelectric textile of 2 × 3 cm^2 area we used as substrates commercial woven fabrics, namely, thin cotton (tnC), thick cotton (tkC) and polyester (PE), which photo presented in Fig. 1(a). To make CuI thin film coatings we employed SILAR modes described earlier in [20–22]. Briefly, we used aqueous solution containing 0.1 M $CuSO_4$ and 0.1 M $Na_2S_2O_3$ as a cationic precursor, into which textile substrates immersed for 20 s. Then, the substrates rinsed in distilled water for 10 s. After that, the fabrics were immersed for 20 s into aqueous NaI solution (anionic precursor), which concentration was 0.05, 0.075 or 0.1 M to carry out the reaction of strongly adsorbed Cu^+ ions on the fiber surfaces and inside the fibers with I^- ions to obtain CuI. The final stage of one SILAR cycle was a rinsing in the distilled water for 10 s for a washing out textiles. Such SILAR cycles for the CuI deposition onto fabric repeated 40 or 80 times.

Morphology of these woven fabrics and thin films CuI deposited on their fibers was observed by scanning electron microscopy (SEM) in a secondary electron mode as in Refs. [20–22]. SEM instrument “Tescan

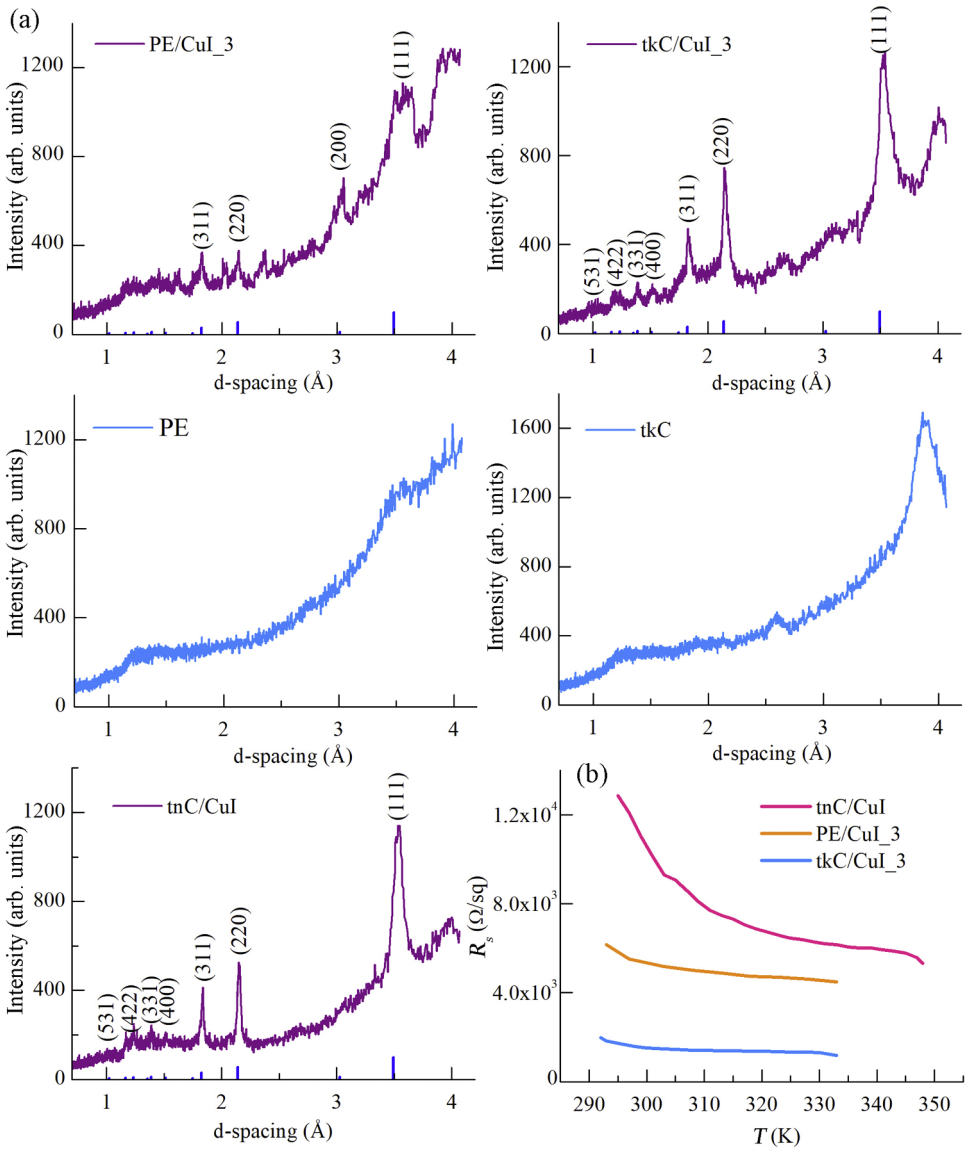

Fig. 5. XRD patterns (a) and plots of sheet resistance R_s versus temperature T (b) for three samples of thermoelectric textiles with CuI coatings obtained by means of 40 cycles of the SILAR method using anionic precursor 0.1 M NaI onto thick cotton (sample tkC/CuI_3), polyester (sample PE/CuI_3) and thin cotton (sample tnC/CuI). For comparison, X-ray diffraction patterns of pure tissues are also shown in (a).

Vega 3 LMH" operated at an accelerating voltage 30 kV without the use of additional conductive coatings, when scanning conductive CuI coated textiles. However, for morphology studies by SEM of the pure fabric we used thin Cr film (~10–15 nm thick) as conductive coating, which evaporated in vacuum at 10^{-4} Pa residual gas pressure immediately before SEM research. Chemical analysis of the pure fabrics and of the samples from series tkC/CuI, PE/CuI, and tnC/CuI was carried out by X-ray fluorescence (XRF) microanalysis using an energy dispersive spectrometry (EDS) system "Bruker XFlash 5010". Energy dispersion spectra were taken from the 50 × 50 μm areas. Quantification of the spectra was carried out in the self-calibrating detector mode.

To analyze crystal structure, we recorded X-ray diffraction (XRD) patterns by a "DRON-4" diffractometer with Bragg–Brentano focusing (theta – 2 theta). The crystalline phases were identified by comparing the experimental diffraction patterns with the reference database JCPDS by using PCPDFWIN v.1.30 software. Average crystallite size D of CuI was determined from the X-ray line broadening method using the Scherer's formula as in Ref. [20]. Calculation of the CuI lattice parameter a was performed in the presence of a sufficient number of diffraction peaks (more than four) in the XRD pattern by the method of least squares using the "UnitCell" program. Crystal lattice microstrains we obtained from the relation $\varepsilon = \Delta d/d$ (where d is the crystal interplanar spacing according to JCPDS, and Δd is the difference between the corresponding experimental and reference interplanar spacing), and dislocation density evaluated through $1/D^2$ as in Ref. [20].

Optical spectra of diffuse reflectance $R(\lambda)$ of the CuI coatings deposited via SILAR on the fabrics were studied for the different tkC/CuI, PE/CuI, and tnC/CuI samples using spectrophotometer "SF-2000" equipped with reflection attachment "SFO-2000". Optical reflection measurements were performed at light incidence angle $\vartheta = 8°$ relative to normal to the surface. Optical band gaps E_g for direct allowed transitions in the CuI films were determined as described in [23] from the Kubelka–Munk function:

$$F(R) = \frac{(1-R)^2}{2R}. \quad (1)$$

As shown in [23], a plot of $(F(R)\cdot h\nu)^2$ vs $h\nu$ yields a direct band gap value E_g of the CuI by extrapolating of $(F(R)\cdot h\nu)^2$ linear part on $h\nu$.

By means of the conventional hot probe method [24] we determined

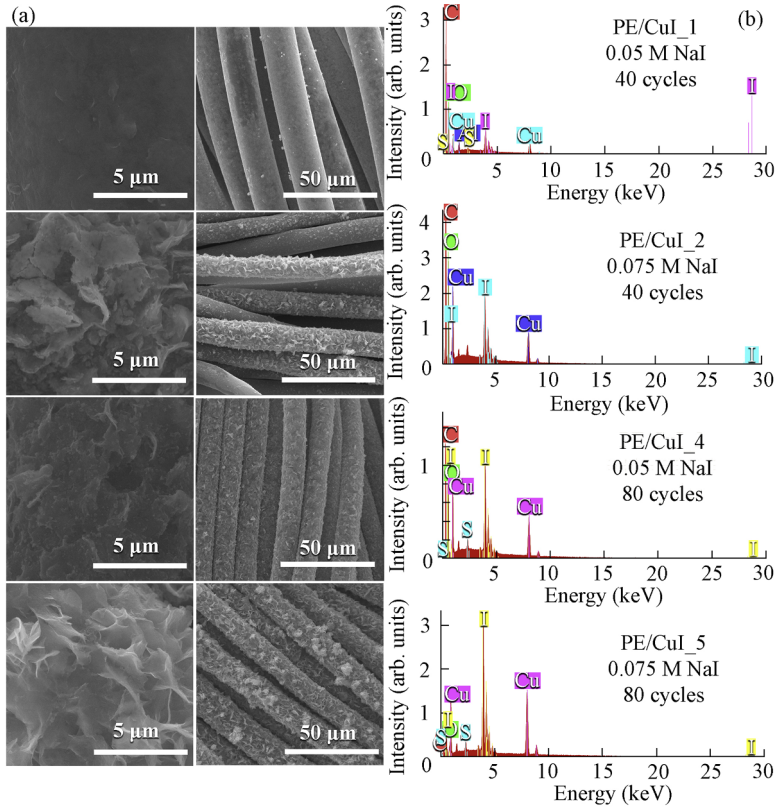

Fig. 6. SEM images (a) and XRF spectra (b) for four samples of thermoelectric textiles with CuI coatings obtained on polyester via SILAR method by means of 40 or 80 cycles using 0.05 M or 0.075 M NaI anionic precursor.

p-type conductivity of the all CuI semiconductor films deposited via SILAR on the different fabrics. Sheet resistance R_s of CuI layers in the different tkC/CuI, PE/CuI, and tnC/CuI samples was obtained by means conventional measurement four-point in-line probe method using a homemade setup described in [23] as four-point collinear probe resistivity ρ measurement system, since $\rho = R_s \times$ film thickness [25]. The measurements were carried out in the near-room temperature range ~ 295 − 335 K. Sheet resistance values calculated according to [23,25] as follows:

$$R_s = F \cdot \frac{\pi}{\ln 2} \cdot \frac{V}{I}, \tag{2}$$

where V is the voltage between the second and third probe measured with a high-impedance voltmeter; I is the constant current between the first and fourth probes; F is a correction factor for the accounting the ratio of the distance between the probes and the size of the thermoelectric textile; $\pi F/\ln 2 \approx 2.35$.

For a measurement of the Seebeck coefficient we used a homemade four-point Seebeck system shown in [23], in which TE textile was suspended in the air between gold ring contacts, which were set at a distance 2.3 cm between hot plate of the Peltier module that act as a heat source, and cold aluminum plate as a sink. According to [26], four-point design reduces the effect of thermal contact resistance. To ensure good thermal contact between the thermocouples and the sample surface, they were glued to the TE textile with a thermally conductive/electrically insulative epoxy adhesive EP30AN-1. The thermocouple ceramic tubes were heat-sunk into the epoxy adhesive, thereby reducing cold-finger effects, when the thermocouples can draw heat away from the sample leading to a temperature difference across the thermocouple bead [26]. The Seebeck coefficient of TE textile was found from the slope of the ΔV vs. ΔT.

In accordance with [19], V_{out} and P_{out} of the single thermoelectric textile *p*-leg in the form of fabric strip of 3 cm long and 0.5 cm wide coated by CuI were obtained as functions of I_{out} for several ΔT in the 5–50 K range, thermoelectric *IV*-characteristics and power-current characteristics, respectively. From V_{out} plotted against I_{out} we obtained values of V_{oc} at load resistance $R_{load} = \infty$, and short circuit current I_{sc}, when $R_{load} = 0$. For electrical connection of the single TE textile *p*-leg through two copper wires with a multimeter we used silver-filled conductive epoxy adhesive “Kontaktol”, and thus obtained ohmic CuI/Ag contacts. The ohmic nature of the CuI/Ag contacts was confirmed by linear current–voltage characteristics with low contact resistances.

Based on the results of studies, three most effective samples of these thermoelectric textiles selected, and experimental designs of flexible wearable TEGs manufactured. For every TEG we used four strips of CuI coated fabrics of (0.5 × 3) cm^2 area each as *p*-type thermoelectric legs. We connected them electrically in series with thin Alumel wires as *n*-type thermoelectric legs and placed on the surface of pure thick cotton fabric. For electrical connection, we used “Kontaktol” and obtained ohmic CuI/Ag and Alumel/Ag contacts. The ohmic nature of the Alumel/Ag contacts was confirmed by linear current–voltage characteristics with low contact resistances. Output parameters (P_{out}, V_{oc} and I_{sc}) of the fabricated flexible in-plane TEGs were obtained, when connecting *n*- and *p*-type thermoelectric legs thermally in parallel on the surface of pure thick cotton fabric at near room temperatures, if ΔT between opposite hot and cold Ag electrodes in the thermoelectric textile in the 5–50 K range was provided by resistive heating of the hot Ag contact with a Peltier module.

In accordance with [16,17,21,22], internal electrical resistance R_{int} of the single *p*-CuI thermoelectric legs and of the wearable textile TEGs was calculated from the corresponding thermoelectric *IV*-characteristics and from P_{out} vs. I plots by equation:

$$R_{\text{int}} = V_{oc}^2/4P_{max}. \tag{3}$$

Accordingly, maximum output power per unit area, i.e. specific output power P^*_{max} (in nW/m^2) was evaluated for the obtained *p*-type

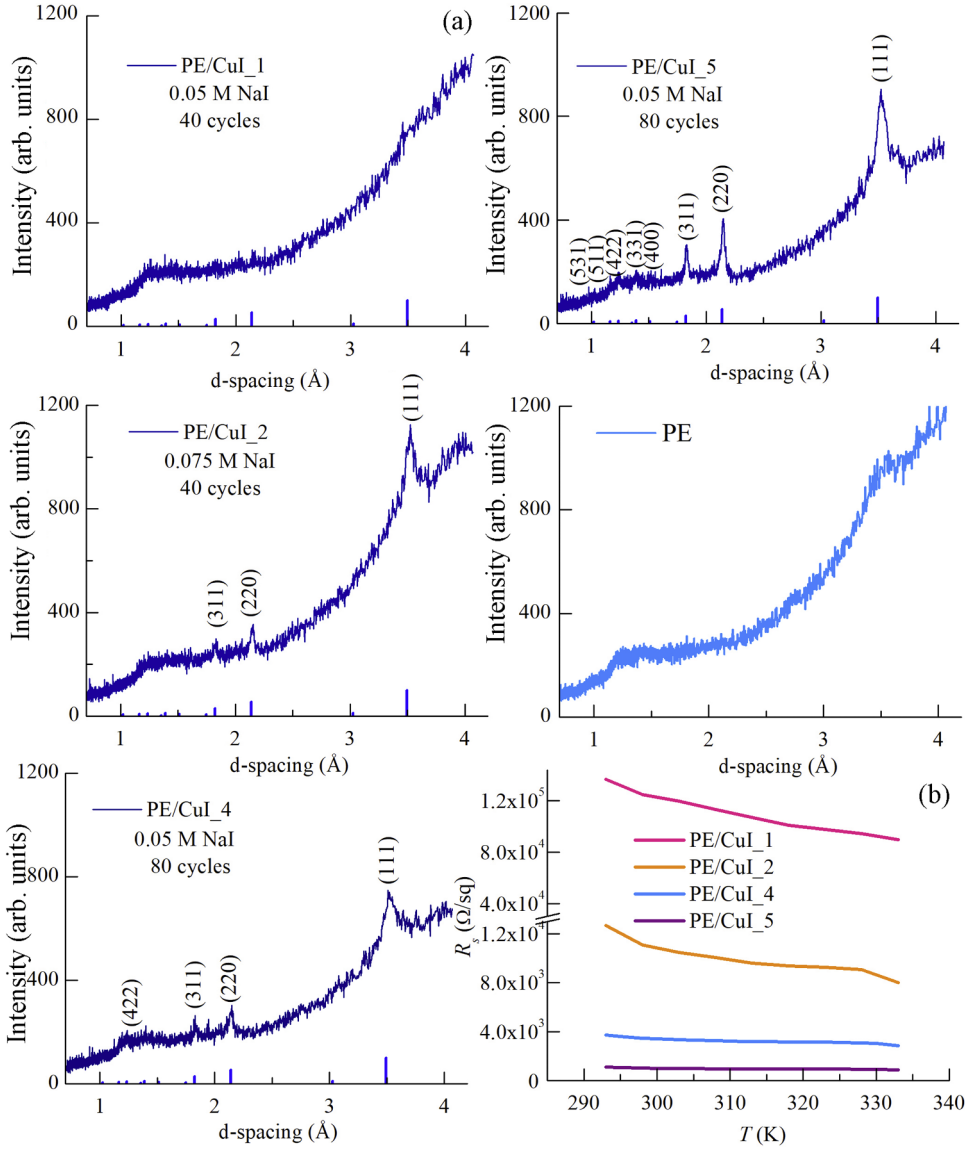

Fig. 7. XRD patterns and plots of sheet resistance R_s versus temperature T for four samples of thermoelectric textiles with CuI coatings obtained on polyester via SILAR method by means of 40 or 80 cycles using 0.05 M or 0.075 M NaI anionic precursor.

CuI single thermoelectric leg as $P^*_{max} = P_{max}/(0.5 \times 3)\cdot 10^{-4}$.

3. Results and discussion

As seen in Fig. 1, the fabrics we selected differ significantly in woven density. In addition, Fig. 2 shows that the structures of the fibers in the tissues are also very dissimilar. The natural cotton samples in Fig. 2(a) are woven from the fibers of complex shape with rough surface, while the smooth cylindrical shape of the fibers is typical for the synthetic polyester fabric in Fig. 2(b). Fig. 2 contains also the corresponding XRF spectra. Note that Cr in the XRF spectra belongs to the electrically conductive chromium film and is not a part of tissues. Chemical compositions of these fabrics obtained by the EDS microanalysis presented in Table 1.

Thermoelectric textiles were made using these fabrics. Table 2 shows manufacturing modes for all obtained samples of thermoelectric textiles with fibers coated by thin CuI films. Optical diffuse reflection spectra in Fig. 3(a) confirm the significant reflectance in the entire visible range for the pure fabrics and also for the thermoelectric textiles with fibers coated by CuI. As seen in Fig. 3(b), band gaps E_g for direct optical transitions in the CuI coatings deposited via SILAR are in the 2.9–3.0 eV range, which is close to typical for CuI [15,17–22]. Based on the band gap data, the formation of this wide-gap semiconductor on the surface of the fibers is confirmed. X-ray diffraction analysis has revealed that all samples presented in Table 2 contain single-phase and polycrystalline coatings with cubic copper iodide crystal structure (zinc-blende, γ-CuI, JCPDS #06–0246).

It was shown in our previous works [21–22], that thickness of CuI films prepared by the SILAR method naturally increases with increasing number of cycles, and also with concentration of the anionic precursor from 0.05 M to 0.1 M NaI. For example, for copper iodide films made in the same modes on poly(ethylene terephthalate) substrates in [22], the CuI film thickness increased from 0.1 to 0.82 μm at 40 SILAR cycles when concentration of the anionic precursor enhanced from 0.05 to 0.1 M NaI. Here we found that the material of the tissue substrate makes a significant contribution to the change in the morphology and properties of copper iodide films obtained via SILAR. Fig. 4 shows SEM images and XRF spectra for three thermoelectric textiles with thickest CuI coatings for each of three types of fabric, obtained by means of 40 cycles of the SILAR method using anionic precursor 0.1 M NaI. We can see in Fig. 4(a), that the outer and inner fibers of all tissues are equally coated with CuI films. According to SEM images with higher

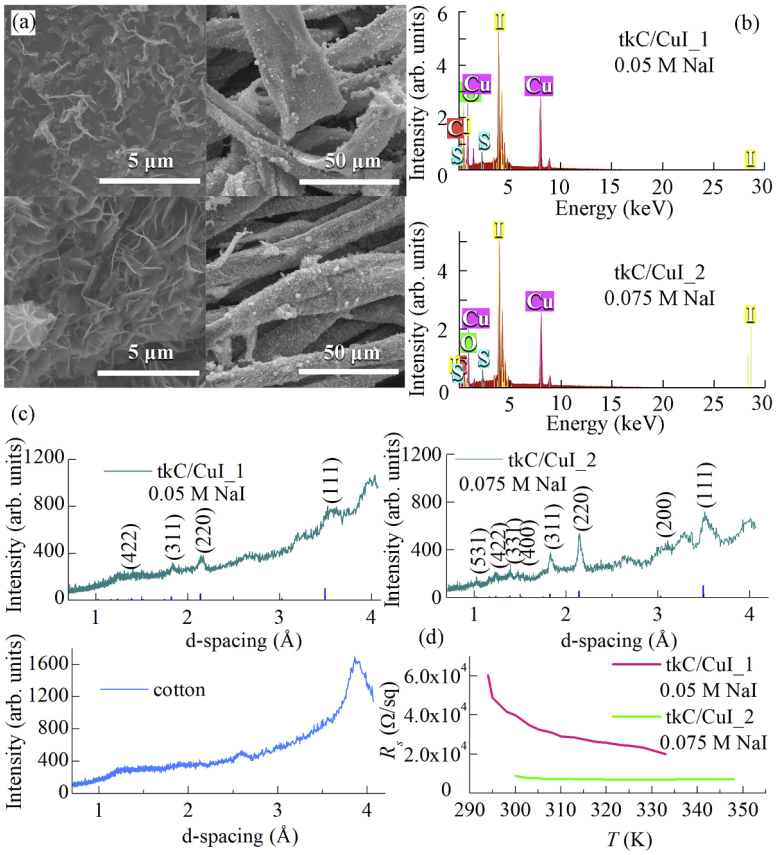

Fig. 8. SEM images (a), XRF spectra (b), XRD patterns (c) and plots of sheet resistance R_s versus temperature T (d) for two samples of thermoelectric textiles with CuI coatings obtained on thick cotton via SILAR method by means of 40 cycles using 0.05 M or 0.075 M NaI anionic precursor.

Table 4
Crystal structure data for CuI coatings in the thermoelectric textiles according to their X-ray diffraction patterns.

Structure parameter	Thermoelectric textile sample on fabric								
	Cotton				Polyester				
	tkC/CuI_1	tkC/CuI_2	tkC/CuI_3	tnC/CuI	PE/CuI_1	PE/CuI_2	PE/CuI_3	PE/CuI_4	PE/CuI_5
D, nm	6–12	11–13	8–13	16–17	–	11–14	14–24	9–11	12
$\varepsilon \cdot 10^3$, a. u.	15–16	10–14	12–14	6–11	–	7–16	5–13	10–20	15
$1/D^2$, nm^{-2}	0.007–0.028	0.006–0.008	0.006–0.016	0.003–0.004	–	0.005–0.008	0.002–0.005	0.008–0.012	0.007
a, Å	–	6.052	6.072	6.075	–	–	–	–	6.067

(according to JCPDS #06–0246, a = 6.051 Å).

resolution in Fig. 4(a), these films are not smooth, especially on thick cotton and on polyester, and are composed of accreted flakes with nanoscale thickness (< 50 nm) or of nanowalls. Chemical X-ray fluorescence microanalysis (Fig. 4(b), Table 3) shows, that all CuI films contain sulfur from the chemically unstable compound sodium thiosulfate $Na_2S_2O_3$ in the cationic precursor that is typical for CuI films fabricated on different substrates by the SILAR method using such solutions [20–22]. As the comparison of the chemical composition of the samples tkC/CuI_3, tnC/CuI and PE/CuI_3 in Table 3 shows, the thinnest is the CuI film, which deposited on the polyester fabric, because the percentage of copper and iodine atoms in the sample PE/CuI_3 is the smallest, compared to C and O, which are related to the PE substrate. The lower content of Cu and I atoms in the sample tnC/CuI compared to the sample tkC/CuI_3 is explained by the lesser tissue density. As confirmation of this, XRD patterns in Fig. 5(a) demonstrate much more intense peaks of γ-CuI X-ray diffractions (JCPDS #06–0246) in the both samples on the cotton fabrics tkC/CuI_3 and tnC/CuI, as compared with PE/CuI_3.

Data on the surface morphology, chemical composition, and crystal structure of the copper iodide layers in all other samples of thermoelectric textiles are shown in Figs. 6–8 and in Tables 3–4. They demonstrate a general increase in the CuI film thickness for all samples with increasing concentration of the anionic precursor and the number of SILAR cycles. In addition, the looser and rough structure of the cotton fabrics than the polyester one contributes to the buildup of more thermoelectric material CuI. For example, the X-ray diffraction of the thinnest sample PE/CuI_1 in Fig. 7 does not have CuI peaks, and the sheet resistance of this sample is the largest. It is seen in Table 4 that all CuI films have a similar crystalline structure. They are nanocrystalline, contain a significant number of dislocations and an increased lattice parameter a, and consequently have large compression microstrains ε. Values of D less than 50 nm obtained on the base of XRD data presented in Table 4 correspond to the thickness of the CuI flakes and nanowalls shown in the SEM images in Figs. 4(a), 6(a), and 8(a).

With that, plots of R_s vs. T in Figs. 5(b), 7(b) and 8(d) show that among the samples of the cotton-based thermoelectric textile the sample tnC/CuI with copper iodide layer on thin cotton fibers has the greatest resistance. Apparently, the loose structure of the tnC fabric prevents the movement of charge carriers in the CuI coating, despite the significant thickness of the copper iodide layer. The temperature

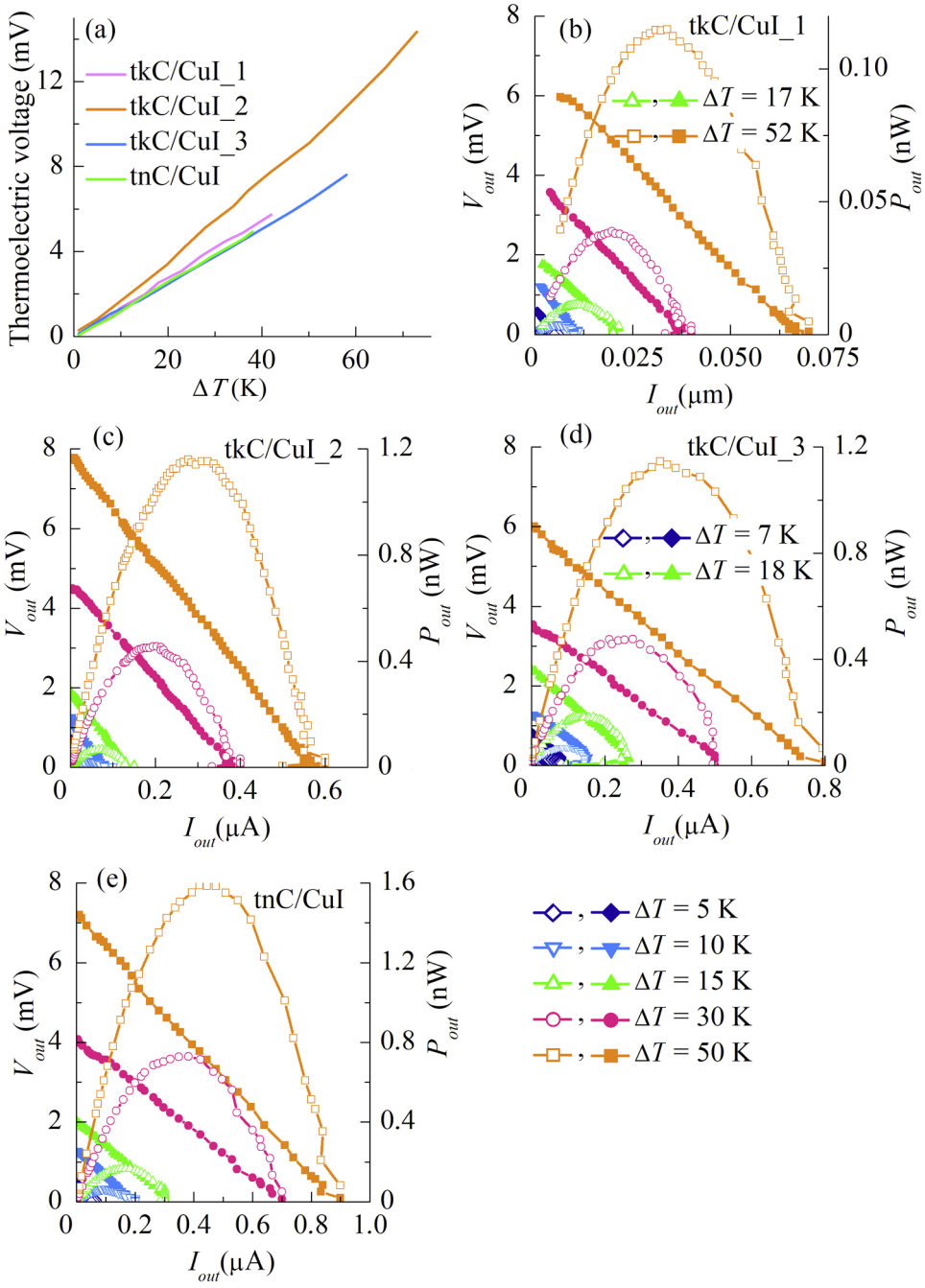

Fig. 9. Thermoelectric voltages induced in response to the temperature gradients ΔT along the thermoelectric textiles with CuI coated cotton (a) and the corresponding plots of output voltage V_{out} (solid symbols) and output power P_{out} (opened symbols) for some temperature gradients ΔT versus output current I_{out}, for the single *p*-CuI thermoelectric legs with an area of (0.5 × 3) cm^2 each in the thermoelectric textile: tkC/CuI_1 (b); tkC/CuI_2 (c); tkC/CuI_3 (d); tnC/CuI (e).

dependences of R_s in Figs. 5(b), 7(b) and 8(d) show unusual transport properties of the *p*-type CuI thin films in TE textiles. In [27,29–31] the same crossover from semiconducting to metallic behavior with increasing temperature, which cannot be explained by thermal activation of the carriers, and a typical ρ minimum in the temperature-dependent resistivity graph have been shown for nanocrystalline CuI thin films obtained through different techniques. According to [27,30], the semiconductor carrier transport occurs in the nanocrystalline CuI films through nearest neighboring hopping. As indicated in [27], when in the CuI thin films the nearest neighbor hopping distance > > Bohr exciton radius (CuI Bohr exciton radius is 1.5 nm [28]) the hopping energy is lesser than the activation energy required for the thermally activated transition of charge carriers to the valence band. Such conduction mechanism has been observed for the thermally evaporated cubic cuprous iodide films [27] and for CuI films deposited via SILAR on PET and glass substrates [29] at near-room temperatures. At elevated temperatures metallic transport in CuI films carried out in accordance with the ionized impurity scattering and the carrier–carrier scattering model for degenerate semiconductors [27,29–31].

At the same time, we took into account that in order to reduce the resistance of the samples from the PE/CuI series, it is necessary to increase the thickness of the CuI coatings by increasing the number of SILAR cycles. Figs. 6 and 7 present an effect of the number of SILAR cycles on the morphology, structure and properties of the thermoelectric polyester-based textiles PE/CuI with CuI coatings deposited using lesser concentrations of the anionic precursor NaI. Fig. 8 shows

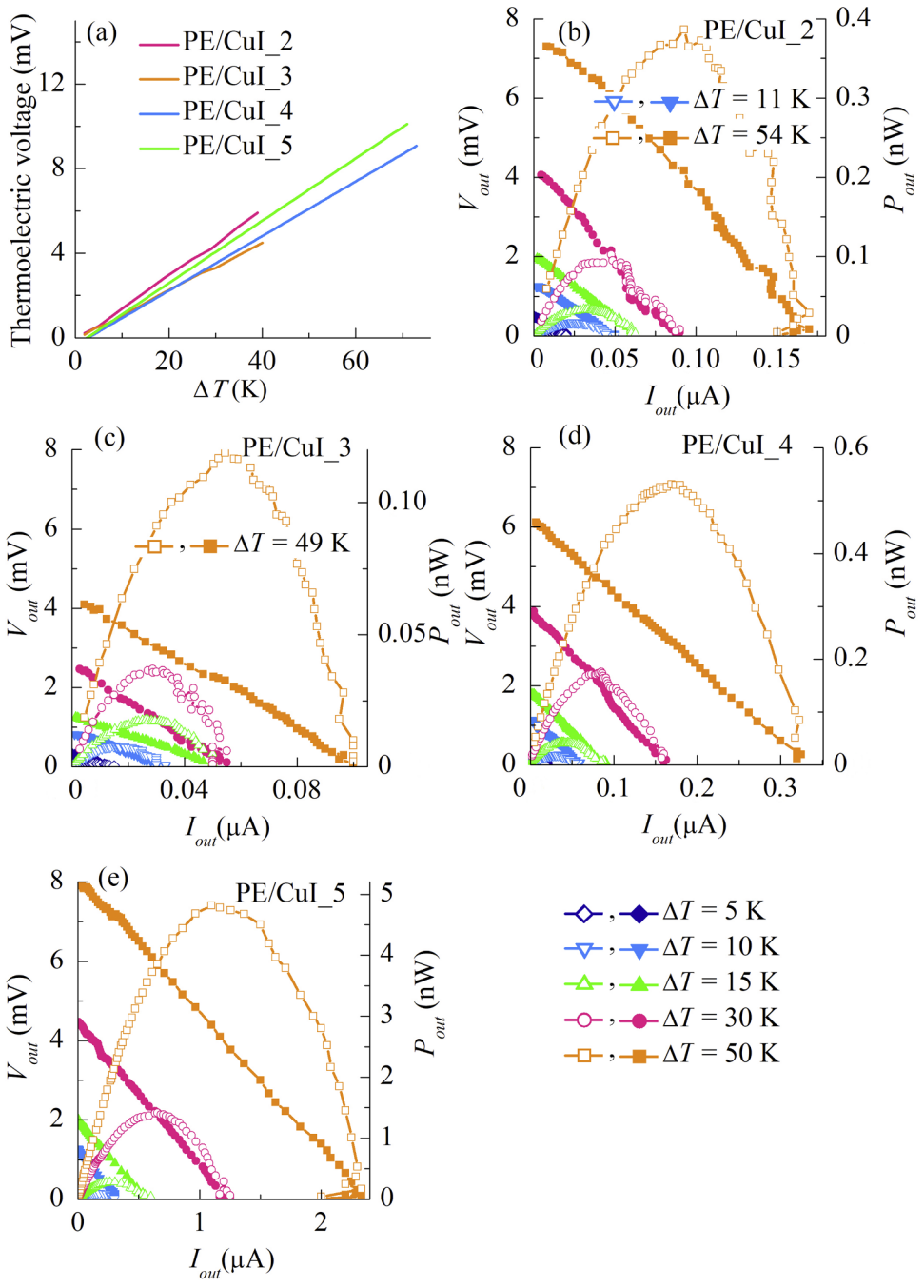

Fig. 10. Thermoelectric voltages induced in response to the temperature gradients ΔT along the thermoelectric textiles with CuI coated polyester (a) and the corresponding plots of output voltage V_{out} (solid symbols) and output power P_{out} (opened symbols) for some temperature gradients ΔT versus output current I_{out}, for the single *p*-CuI thermoelectric legs with an area of (0.5 × 3) cm^2 each in the thermoelectric textile: PE/CuI_2 (b); PE/CuI_3 (c); PE/CuI_4 (d); PE/CuI_5 (e).

similar data for cotton-based textiles tkC/CuI. It can be seen that the most electrically conductive among all the samples are tkC/CuI_3, PE/CuI_4 and PE/CuI_5 with R_s in the range (1–4) × 10^3 Ω/sq.

According to the graphs of the thermoelectric voltages induced in response to the temperature gradients along the thermoelectric textiles with CuI coated cotton (Fig. 9) and polyester (Fig. 10) we have determined the values of the Seebeck coefficient in the range of 130–180 μV K^{-1} irrespective of the fabric. Note that *S* for all samples is constant in the temperature range 290–365 K.

Plots of the output voltages and output powers versus output currents obtained for the single *p*-CuI thermoelectric legs with an area of (0.5 × 3) cm^2 each, made from the thermoelectric textiles are shown in Figs. 9 and 10. According to [19,21,22], the open circuit voltage for such single-leg thin film thermoelectric modules is described by the equation $V_{oc} = S\Delta T$. The values of the Seebeck coefficient calculated from this ratio using thermoelectric *IV*-characteristics are in the range of 120–160 μV K^{-1} regardless of temperature gradient, with the exception of the sample PE/CuI_3, which $S \approx 85$ μV K^{-1}. These values of the Seebeck coefficient coincide with the *S* values obtained from the slope of the ΔV vs. ΔT within the experimental error. The comparison of the Seebeck coefficients confirms the ohmic nature of the silver-filled conductive epoxy adhesive "Kontaktol" contacts to the thermoelectric textile we have made. As can be seen in Fig. 10(a), the sample PE/CuI_3 has the smallest value $S \approx 105$ μV K^{-1}. The difference in the Seebeck coefficient values obtained by different methods for single *p*-CuI thermoelectric leg PE/CuI_3 can probably be explained by the insufficient

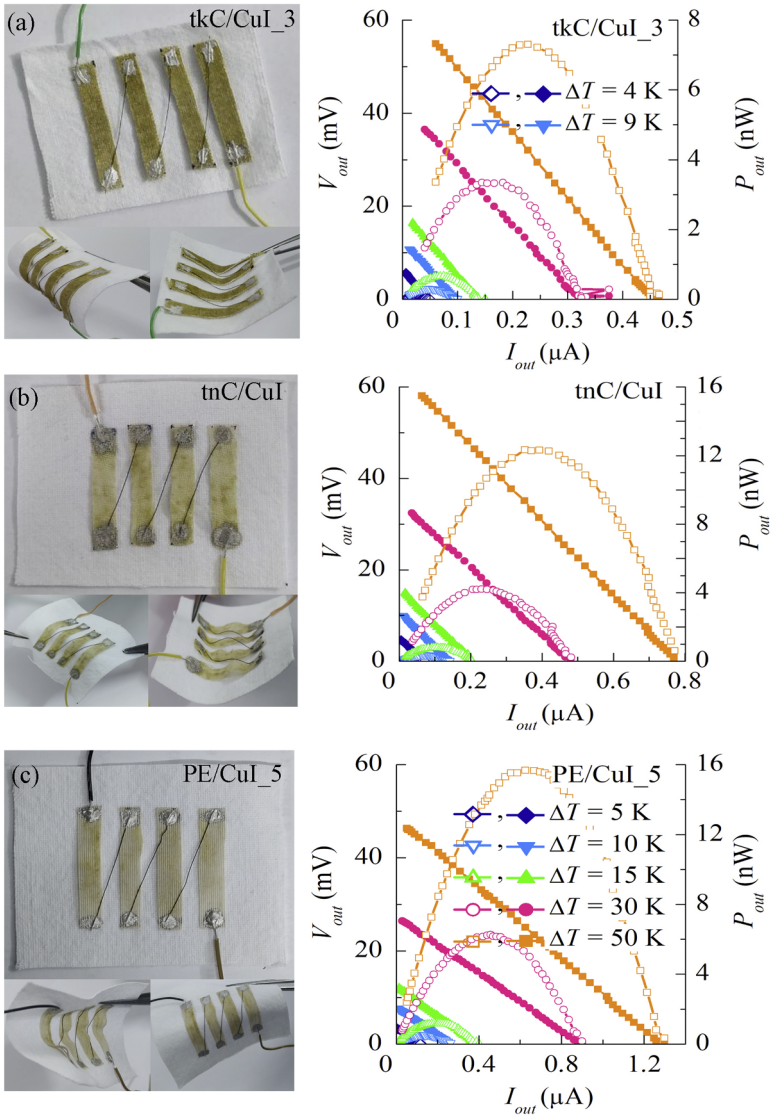

Fig. 11. Photos of three wearable textile TEGs having four thermoelectric textile strips each and their output voltage V_{out} (solid symbols) and output power P_{out} (opened symbols) for some temperature gradients ΔT versus output current I_{out}: (a) – TEG based on tkC/CuI_3; (b) – TEG based on tnC/CuI_3; (c)–TEG based on PE/CuI_5.

thickness of the copper iodide layer according to XRF data in Fig. 4(b) and EDS values of Cu and I in Table 3.

Figs. 9, 10 show good output characteristics V_{oc}, I_{sc} and P_{out} for single *p*-CuI thermoelectric legs in the samples tkC/CuI_2, tkC/CuI_3, PE/CuI_4 and tnC/CuI. The single *p*-CuI thermoelectric leg made from textile sample PE/CuI_5 demonstrates the best V_{oc}, I_{sc} and P_{out}.

The obtained at $\Delta T \approx 50$ K specific output powers of the *p*-type CuI single thermoelectric legs were $P^*_{max} \approx 7$ μW/m^2 for tkC/CuI_2 and tkC/CuI_3, $P^*_{max} \approx 10$ μW/m^2 for tnC/CuI, $P^*_{max} \approx 9$ μW/m^2 for PE/CuI_3, $P^*_{max} \approx 4$ μW/m^2 for PE/CuI_4, and $P^*_{max} \approx 31$ μW/m^2 for PE/CuI_5. It turned out that the larger thickness of the copper iodide layers on the tissues does not always provide them with thermoelectric efficiency. Probably, the lower density of the thin cotton and polyester fabrics provide reduced thermal conductivity, which determines their good thermoelectric output characteristics. In addition, as shown by calculations of the internal resistance of these samples according to Eq. (3), the output characteristics are better at low R_{int} values. For example, single *p*-CuI thermoelectric legs in tkC/CuI_2 and in PE/CuI_4 have $R_{int} \approx 15$ kΩ, and R_{int} of tkC/CuI_3 and tnC/CuI ~ 7 kΩ. The most effective single *p*-CuI thermoelectric leg PE/CuI_5 has $R_{int} \approx 2$ kΩ. Note, that within the experimental error, the internal resistance is almost independent of the temperature gradient in the ΔT range 15 – 50 K, which is in good agreement with the temperature dependences of the surface resistances of TE textiles at $T > 300$ K in Figs. 5(b), 7(b) and 8(d).

Fig. 11 shows photos of three wearable textile TEGs having four thermoelectric textile strips each and their output parameters. The design of TEG is based on the idea of [4] for a manufacturing of wearable all-fabric thermoelectric generator, whose advantage is the ability to incorporate fabric thermopiles into garments. The additional plus of our design compared to that proposed in [4] is the increased output power due to the use of thermoelectric Alumel wires instead of carbon filaments in [4] and thus we created in our design the thermocouples with *p*-CuI and *n*-Alumel branches. Calculations of the internal resistance of these TEGs according to Eq. (3) confirmed the relationship between R_{int} and output characteristics. TEG on the base of tkC/CuI_3 has $R_{int} \approx 120$ kΩ, R_{int} of TEG based on tnC/CuI ~ 70 kΩ, and R_{int} of TEG on PE/CuI_5 does not exceed 40 kΩ. It is seen in Fig. 11, that the best TEG obtained on the polyester fabric has $V_{oc} = 44$ mV, $I_{sc} = 1.3$ μA, and $P_{out} = 16$ nW at temperature difference 50 K. The other two TEG samples also have good output characteristics, like the best textile TEGs reported in [1,4,6,9,12]. The TEG samples we

fabricated kept the output parameters unchanged after repeated bends more than 50 times in different directions, similar to that shown in the photos in Fig. 11, which confirms their favorable mechanical performance.

4. Conclusions

Via low-temperature cheap and scalable method SILAR we have deposited copper iodide thin films onto commercial cotton and polyester fabrics and so obtain different samples of thermoelectric textiles, in which CuI coat all fibers on both sides and in the middle of the fabric, and even inside the fibers. The CuI films are composed of accreted flakes with nanoscale thickness (< 50 nm) or of nanowalls. Their crystal grains are less than 50 nm, contain a significant number of dislocations and an increased lattice parameter, and consequently have large compression microstrains. Material of the tissue substrate makes a significant contribution to the change in the morphology and properties of copper iodide films obtained via SILAR. In particular, the looser and rough structure of the cotton fabrics than the polyester one contributes to the buildup of more thermoelectric material CuI with lower sheet resistance. The TE textiles with CuI coated cotton and polyester have the Seebeck coefficients in the range of 120–180 μV K^{-1}, which are constant at the temperatures 290–365 K. The most effective single *p*-CuI thermoelectric leg has low internal resistance 2 kΩ. Its specific output power at temperature gradient 50 K is 31 μW/m^2. Three experimental flexible wearable TEGs of simple and affordable designs having each four thermocouples with *n*-Alumel and *p*-CuI thermoelectric legs on the thick cotton, thin cotton and polyester confirm the possibility of obtaining electricity using the developed TE textiles under conditions of temperature gradients from 5 to 50 K at near-room temperatures. The best TEG obtained on the polyester fabric has at temperature difference 50 K output TE characteristics: V_{oc} = 44 mV, I_{sc} = 1.3 μA, and P_{out} = 16 nW, like the best textile TEGs reported in the literature. These characteristics remain unchanged after repeated bends of TEGs in the different directions. The next stages of research will be a reproducibility of the data presented in this work for a large number of TE textile samples and reliability tests of these TEGs.

CRediT authorship contribution statement

N.P. Klochko: Conceptualization, Methodology, Validation, Writing - original draft. **K.S. Klepikova:** Visualization, Formal analysis, Writing - review & editing. **D.O. Zhadan:** Methodology, Investigation, Formal analysis. **V.R. Kopach:** Methodology, Validation, Writing - review & editing. **S.M. Chernyavskaya:** Writing - review & editing. **S.I. Petrushenko:** Investigation, Writing - review & editing. **S.V. Dukarov:** Investigation, Writing - review & editing. **V.M. Lyubov:** Investigation. **A.L. Khrypunova:** Writing - review & editing.

Declaration of Competing Interest

The authors declare no competing interest.

Acknowledgments

The authors gratefully acknowledge the financial support of Ministry of Education and Science of Ukraine under project number M 5487.

References

[1] Q. Wu, J. Hu, Thermoelectric textile materials, in: P. Aranguren (Ed.), Bringing Thermoelectricity into Reality, IntechOpen, London, 2018, pp. 24–37, , https://doi.org/10.5772/intechopen.75474.
[2] Z. Lu, H. Zhang, C. Mao, C.M. Li, Silk fabric-based wearable thermoelectric generator for energy harvesting from the human body, Appl. Energy 164 (2016) 57–63, https://doi.org/10.1016/j.apenergy.2015.11.038.
[3] Q. Wu, J. Hu, A novel design for a wearable thermoelectric generator based on 3D fabric structure, Smart Mater. Struct. 26 (4) (2017) 045037, , https://doi.org/10.1088/1361-665x/aa5694.
[4] L.K. Allison, T.L. Andrew, A wearable all-fabric thermoelectric generator, Adv. Mater. Technol. 4 (5) (2019) 1800615, , https://doi.org/10.1002/admt.201800615.
[5] L. Wang, K. Zhang, Textile-based thermoelectric generators and their applications, Energy Environ. Mater. 0 (2019) 1–13, https://doi.org/10.1002/eem2.12045.
[6] Y. Du, K. Cai, S. Chen, H. Wang, S.Z. Shen, R. Donelson, T. Lin, Thermoelectric fabrics: toward power generating clothing, Sci. Rep. 5 (1) (2015) 6411, https://doi.org/10.1038/srep06411.
[7] T. Zhang, K. Li, J. Zhang, M. Chen, Z. Wang, S. Ma, N. Zhang, L. Wei, High-performance, flexible, and ultralong crystalline thermoelectric fibers, Nano Energy 41 (2017) 35–42, https://doi.org/10.1016/j.nanoen.2017.09.019.
[8] S. Shin, R. Kumar, J.W. Roh, D.-S. Ko, H.-S. Kim, S.I. Kim, L. Yin, S.M. Schlossberg, S. Cui, J.-M. You, S. Kwon, J. Zheng, J. Wang, R. Chen, High-performance screen-printed thermoelectric films on fabrics, Sci. Rep. 7 (1) (2017) 7317, https://doi.org/10.1038/s41598-017-07654-2.
[9] L. Zhang, S. Lin, T. Hua, B. Huang, S. Liu, X. Tao, Fiber-based thermoelectric generators: materials, device structures, fabrication, characterization, and applications, Adv. Energy Mater. 8 (5) (2018) 1700524, , https://doi.org/10.1002/aenm.201700524.
[10] Y. Jia, L. Shen, J. Liu, W. Zhou, Y. Du, J. Xu, C. Liu, Z. Ge, Z. Zhang, F. Jiang, An efficient PEDOT-coated textile for wearable thermoelectric generators and strain sensors, J. Mater. Chem. C 7 (12) (2019) 3496–3502, https://doi.org/10.1039/c8tc05906c.
[11] S. Hong, Y. Gu, J.K. Seo, J. Wang, P. Liu, Y.S. Meng, S. Xu, R. Chen, Wearable thermoelectrics for personalized thermoregulation, Sci. Adv. 5 (5) (2019) eaaw0536, https://doi.org/10.1126/sciadv.aaw0536.
[12] M. Ito, T. Koizumi, H. Kojima, T. Saito, M. Nakamura, From materials to device design of a thermoelectric fabric for wearable energy harvesters, J. Mater. Chem. A 5 (24) (2017) 12068–12072, https://doi.org/10.1039/c7ta00304h.
[13] M. Jung, S. Jeon, J. Bae, Scalable and facile synthesis of stretchable thermoelectric fabric for wearable self-powered temperature sensors, RSC Adv. 8 (70) (2018) 39992–39999, https://doi.org/10.1039/c8ra06664g.
[14] D.M. Rowe, Thermoelectrics Handbook: Macro to Nano, 1st ed., CRC Press, Boca Raton, 2006, https://doi.org/10.1201/9781420038903.
[15] J. Coroa, B.M. Morais Faustino, A. Marques, C. Bianchi, T. Koskinen, T. Juntunen, I. Tittonen, I. Ferreira, Highly transparent copper iodide thin film thermoelectric generator on a flexible substrate, RSC Adv. 9 (2019) 35384–35391, https://doi.org/10.1039/c9ra07309d.
[16] Y. Du, J. Xu, B. Paul, P. Eklund, Flexible thermoelectric materials and devices, Appl. Mater. Today 12 (2018) 366–388, https://doi.org/10.1016/j.apmt.2018.07.004.
[17] B.M. Morais Faustino, D. Gomes, J. Faria, T. Juntunen, G. Gaspar, C. Bianchi, A. Almeida, A. Marques, I. Tittonen, I. Ferreira, CuI p-type thin films for highly transparent thermoelectric p-n modules, Sci. Rep. 8 (1) (2018) 6867, https://doi.org/10.1038/s41598-018-25106-3.
[18] N. Yamada, R. Ino, H. Tomura, Y. Kondo, Y. Ninomiya, High-mobility transparent p-type CuI semiconducting layers fabricated on flexible plastic sheets: toward flexible transparent electronics, Adv. Electron. Mater. 3 (12) (2017) 1700298, , https://doi.org/10.1002/aelm.201700298.
[19] C. Yang, D. Souchay, M. Kneiß, M. Bogner, H.M. Wei, M. Lorenz, O. Oeckler, G. Benstetter, Y.Q. Fu, M. Grundmann, Transparent flexible thermoelectric material based on non-toxic earth-abundant p-type copper iodide thin film, Nat. Commun. 8 (2017) 16076, https://doi.org/10.1038/ncomms16076.
[20] N.P. Klochko, K.S. Klepikova, V.R. Kopach, D.O. Zhadan, V.V. Starikov, D.S. Sofronov, I.V. Khrypunova, S.I. Petrushenko, S.V. Dukarov, V.M. Lyubov, M.V. Kirichenko, S.P. Bigas, A.L. Khrypunova, Solution-produced copper iodide thin films for photosensor and for vertical thermoelectric nanogenerator, which uses a spontaneous temperature gradient, J. Mater. Sci. 30 (18) (2019) 17514–17524, https://doi.org/10.1007/s10854-019-02103-4.
[21] N.P. Klochko, K.S. Klepikova, V.R. Kopach, I.I. Tyukhov, D.O. Zhadan, G.S. Khrypunov, S.I. Petrushenko, S.V. Dukarov, V.M. Lyubov, M.V. Kirichenko, A.L. Khrypunova, Semitransparent p-CuI and n-ZnO thin films prepared by low temperature solution growth for thermoelectric conversion of near-infrared solar light, Sol. Energy 171 (2018) 704–715, https://doi.org/10.1016/j.solener.2018.07.030.
[22] N.P. Klochko, D.O. Zhadan, K.S. Klepikova, S.I. Petrushenko, V.R. Kopach, G.S. Khrypunov, V.M. Lyubov, S.V. Dukarov, A.L. Khrypunova, Semi-transparent copper iodide thin films on flexible substrates as p-type thermolegs for a wearable thermoelectric generator, Thin Solid Films 683 (2019) 34–41, https://doi.org/10.1016/j.tsf.2019.05.025.
[23] N.P. Klochko, V.R. Kopach, I.I. Tyukhov, G.S. Khrypunov, V.E. Korsun, V.O. Nikitin, V.M. Lyubov, M.V. Kirichenko, O.N. Otchenashko, D.O. Zhadan, M.O. Maslak, A.L. Khrypunova, Wet chemical synthesis of nanostructured semiconductor layers for thin-film solar thermoelectric generator, Sol. Energy 157 (2017) 657–666, https://doi.org/10.1016/j.solener.2017.08.060.
[24] A. Axelevitch, G. Golan, Hot-probe method for evaluation of majority charged carriers concentration in semiconductor thin films, Facta Universitatis Series: electron, Energetics 26 (2013) 187–195, https://doi.org/10.2298/FUEE1303187a.
[25] H.B. Pan, J.N. Ding, B.G. Cao, G.G. Cheng, Design and evaluation of a high-accuracy measurement system for sheet resistance of thin films, Key Eng. Mater. 609–610 (2014) 106–112, https://doi.org/10.4028/www.scientific.net/kem.609-610.106.
[26] S. Iwanaga, E.S. Toberer, A. LaLonde, G.J. Snyder, A high temperature apparatus for measurement of the seebeck coefficient, Rev. Sci. Instrum. 82 (2011) 063905, ,

https://doi.org/10.1063/1.3601358.
[27] D.K. Kaushik, M. Selvaraj, S. Ramu, A. Subrahmanyam, Thermal evaporated Copper Iodide (CuI) thin films: a note on the disorder evaluated through the temperature dependent electrical properties, Sol. Energy Mater. Sol. Cells 165 (2017) 52–58, https://doi.org/10.1016/j.solmat.2017.02.030.
[28] Y. Yang, L. Shuman, K. Keisaku, Synthesis of well-dispersed CuI nanoparticles from an available solution precursor, Chem. Lett. 34 (8) (2005) 1158–1159, https://doi.org/10.1246/cl.2005.1158.
[29] N.P. Klochko, K.S. Klepikova, D.O. Zhadan, V.R. Kopach, Y.R. Kostyuchenko, I.V. Khrypunova, V.M. Lyubov, M.V. Kirichenko, A.L. Khrypunova, S.I. Petrushenko, S.V. Dukarov, Transport properties of cubic cuprous iodide films deposited by successive ionic layer adsorption and reaction, Microstructure and Properties of Micro- and Nanoscale Materials, Films, and Coatings (NAP 2019), 240 Springer Proceedings in Physics, 2020, pp. 19–30, , https://doi.org/10.1007/978-981-15-1742-6_3.
[30] M. Kneiß, C. Yang, J. Barzola-Quiquia, G. Benndorf, H. von Wenckstern, P. Esquinazi, M. Lorenz, M. Grundmann, Suppression of grain boundary scattering in multifunctional p-type transparent γ-CuI thin films due to interface tunneling currents, Adv. Mater. Interfaces 5 (6) (2018) 1701411, , https://doi.org/10.1002/admi.201701411.
[31] C. Yang, M. Kneiβ, M. Lorenz, M. Grundmann, Room-temperature synthesized copper iodide thin film as degenerate p-type transparent conductor with a boosted figure of merit, Proc. Nat. Acad. Sci. 113 (46) (2016) 12929–12933, https://doi.org/10.1073/pnas.1613643113.